
EXTENSION OF THE LANGEVIN POWER CURVE ANALYSIS BY SEPARATION PER OPERATIONAL STATE

Christian Philipp^{1,*}, Henrik M. Bette², Matthias Wächter¹, Jan Freund¹, Thomas Guhr², Joachim Peinke¹

¹
Fakultät V
Carl von Ossietzky University
Oldenburg, Germany

²
Fakultät für Physik
University of Duisburg-Essen
Duisburg, Germany

*
christian.philipp@uni-oldenburg.de

May 26, 2023

ABSTRACT

in the last few years, the dynamical characterization of the power output of a wind turbine by means of a Langevin equation has been well established. For this approach, temporally highly resolved measurements of wind speed and power output are used to obtain the drift and diffusion coefficients of the energy conversion process. These coefficients fully determine a Langevin stochastic differential equation with Gaussian white noise. The drift term specifies the deterministic behavior of the system whereas the diffusion term describes the stochastic behavior of the system. A precise estimation of these coefficients is essential to understand the dynamics of the power conversion process of the wind turbine. We show that the dynamics of the power output of a wind turbine have a hidden dependency on turbine's different operational states. Here, we use an approach based on clustering Pearson correlation matrices for different observables on a moving time window to identify different operational states. We have identified five operational states in total, for example the state of rated power. Those different operational states distinguish non-stationary behavior in the mutual dependencies and represent different turbine control settings. As a next step, we condition our Langevin analysis on these different states to reveal distinctly different behaviors of the power conversion process for each operational state. Moreover, in our new representation hysteresis effects which have typically appeared in the Langevin dynamics of wind turbines seem to be resolved. We assign these typically observed hysteresis effects clearly to the change of the wind energy system between our estimated different operational states. In this contribution, we discuss further consequences for the meaning of hysteric switching and detection of malbehaviors in wind turbines.

1 Introduction

Wind turbines have become a significant source of renewable energy due to their environmentally-friendly nature and potential to generate electricity. Analyzing their energy conversion process can be challenging due to the intricate nature influenced by various factors, including wind speed, turbulence, and mechanical wear. Nonetheless, a precise understanding of the dynamics of wind turbines is critical to simulate and consequently optimize their energy output and detect malfunctions [5].

Recently, the Langevin equation approach [6] has been used to study the dynamics of wind turbines [1] [2]. This approach utilizes temporally highly resolved measurements of wind speed and power output to determine the drift and diffusion coefficients of the energy conversion process, which characterize the deterministic and stochastic behavior

of the system. However, this approach assumes a stationary system and does not account for the potential impact of different operational states.

Authors of a recent study proposed a new approach based on clustering Pearson correlation matrices to identify different operational states of wind turbines [3]. By analyzing different observables over a moving time window, they identified five operational states, which distinguish non-stationary behavior in the mutual dependencies and represent different turbine control settings.

This study employs the method to identify and distinguish various operational states, which are then used to condition the Langevin analysis. The analysis revealed unique behaviors in the power conversion process corresponding to each operational state. The study also successfully resolved hysteresis effects commonly observed in the dynamics of wind turbines [1] [7].

The implications of this research are significant for the optimization of wind turbines' performance and the detection of malfunctions. By identifying different operational states, the authors' approach provides a more comprehensive understanding of the dynamics of wind turbines and can lead to more efficient operation and maintenance. Additionally, resolving hysteresis effects can aid in the detection of malfunctions.

2 Data set

The data utilized in this study is sourced from the Supervisory Control and Data Acquisition (SCADA) system of a Vestas V90 turbine located in the Thanet offshore wind farm. These measurements were recorded at approximately 5-second intervals throughout the year 2017. To ensure consistent time stamps and a stable frequency, the data was aggregated by averaging over 10-second intervals. It is important to note that if no measurements were obtained within the original 5-second interval, the aggregated dataset may contain missing data during the corresponding 10-second interval.

The dataset under analysis comprises six variables, namely:

- ActivePower: Generated active power
- CurrentL1: Generated current (chosen from one of the three phases due to no deviations in the data)
- RotorRPM: Rotations per minute of the rotor
- GeneratorRPM: Rotations per minute of the high-speed shaft at the generator
- BladePitchAngle: Blade pitch angle of the blades
- WindSpeed: Wind speed

Our expectation for the V90 turbine is a shift in control strategy as the wind speed changes. This shift includes transitioning from a low wind speed regime with variable rotation speed, to an intermediate regime with constant rotation, and finally to a rated region with constant rotation and produced power. The selection of these variables allows us to effectively analyze these operational state changes. The inclusion of both rotational speed variables and the addition of current to active power is aimed at maintaining consistency for the study, particularly for identifying of operational states using the correlation matrix. This selection is essential for characterizing correlation structures and detecting any anomalies that may disrupt these structures.

3 Methods

3.1 Correlation matrix states

In order to automatically calculate the operational state of a turbine, we employ a method presented in Bette et. al. [Bette2021]. Pearson correlation matrices are calculated for non-overlapping time intervals called epochs to obtain a time series of correlation matrices. These are clustered to find structurally different operational states and thereby a time series $S(t)$, which offers us the current operational state for every time t .

For this calculation we use all channels presented in sec. ???. Each of these variables is represented by a time series $X_k(t)$, where $k = 1, \dots, K$ represents the different variables and $t = 1, \dots, T_{\text{end}}$ is the time variable in the arbitrary unit of time steps. To capture non-stationarity we separate the whole time series into disjoint intervals ϵ of length $T = 30\text{min}$. The interval length is chosen as a compromise between as short as possible to best resolve non-stationarity and as long as necessary to avoid noise in the correlation coefficients. ϵ represents the starting time of an interval, so that $X_k(t)$, $\epsilon \leq t < \epsilon + T$ is the time series in the interval ϵ .

Next, we normalize each time series in every interval to mean value zero and standard deviation one by

$$G_k(t) = \frac{X_k(t) - \mu_k(\epsilon)}{\sigma_k(\epsilon)} , \quad k = 1, \dots, K , \quad \epsilon \leq t < \epsilon + T , \quad (1)$$

with $\mu_k(\epsilon)$ and $\sigma_k(\epsilon)$ being the mean value and the standard deviation of variable k in interval ϵ respectively. By arranging the variable time series in each epoch in a $K \times T$ data matrix

$$G(\epsilon) = \begin{bmatrix} G_1(\epsilon) & \dots & G_1(\epsilon + T - 1) \\ \vdots & & \vdots \\ G_k(\epsilon) & \ddots & G_k(\epsilon + T - 1) \\ \vdots & & \vdots \\ G_K(\epsilon) & \dots & G_K(\epsilon + T - 1) \end{bmatrix} . \quad (2)$$

we easily calculate the correlation matrix in the interval ϵ

$$C(\epsilon) = \frac{1}{T} G(\epsilon) G^\dagger(\epsilon) . \quad (3)$$

Here, $G^\dagger(\epsilon)$ denotes the transpose of $G(\epsilon)$. Each matrix element $C(\epsilon)_{ij}$ is the Pearson correlation coefficient between the variables i and j in the interval ϵ .

We apply hierarchical k -means clustering to find recurring states in our system. The algorithm is a divisive clustering that splits by applying standard k -means with $k = 2$. In each step, the cluster with the largest internal distance to its own center is split. Hence, we must define a distance $d(\epsilon, \epsilon')$ between the correlation matrices for intervals ϵ and ϵ' :

$$d(\epsilon, \epsilon') = \sqrt{\sum_{i,j} (C_{ij}(\epsilon) - C_{ij}(\epsilon'))^2} = \|C(\epsilon) - C(\epsilon')\| . \quad (4)$$

The center of cluster s is calculated as the element-wise mean

$$\langle C_{ij} \rangle_s = \frac{1}{|z_s|} \sum_{S(\epsilon)=s} C_{ij} \quad (5)$$

with $|z_s|$ as the number of elements in cluster s . $S(t)$ is the function which results in the cluster s for any time stamp t assigned by the algorithm to the interval ϵ that contains t . A more detailed description of the clustering procedure is found in Bette et. al. [3].

3.2 Estimation of the Kramers-Moyal coefficients

The traditional approach to model the power conversion process of a wind turbine in terms of stationary Langevin equation is shown in equation (6). Here, the power output $P(t)$ is modeled as a one-dimensional stationary stochastic process for a fixed wind speed u . We assume a Gaussian distributed, delta correlated noise $\Gamma(t)$ with zero mean and a variance of 2.

$$\dot{P}(t)|_{u(t)=u} = D_P^{(1)}(P(t), u) + \sqrt{D_P^{(2)}(P(t), u)} \cdot \Gamma(t) \quad (6)$$

Analytically, the n 'th conditional moments of the power output $M_P^{(n)}(P, u, \tau)$ can be derived with expected value of the increments $\Delta_\tau P(t) = P(t + \tau_0) - P(t)$ over the time step τ at the specific state (P, u) with equation (7).

$$M_P^{(n)}(P, u, \tau) = \langle (\Delta_\tau P(t))^n \rangle |_{P(t)=P, u(t)=u} \quad (7)$$

With the n 'th conditional moments the n 'th Kramers-Moyal coefficient $D_P^{(n)}(u, P)$ can be calculated [6].

$$D_P^{(n)}(P, u) = \lim_{\tau \rightarrow 0} \frac{M_P^{(n)}(P, u, \tau)}{n! \cdot \tau} \quad (8)$$

We consider a two-dimensional dataset (P, u) with N datapoints with an equidistant sample interval τ_s . Furthermore, we define $\tau_m = m \cdot \tau_s$, where $m \in \mathbb{N}$. With this definition, we can calculate the increments of the power output over a time lag τ_m with equation (9).

$$\Delta_{\tau_m} P_i = P_{i+m} - P_i \quad (9)$$

To estimate the n -th conditional moment $M_P^{(n)}(P, u, \tau_m)$, we employ the Nadaraya-Watson estimator with a two-dimensional kernel $K_{a,b}(x, y) = k_a(x) \cdot k_b(y)$. This kernel can be represented as the product of two one-dimensional kernels. The Nadaraya-Watson estimator functions as a means of calculating the weighted, data-driven average of increments. These weights in our specific case are determined by the states P and u , as well as the kernel functions $k_a(x)$ and $k_b(y)$, along with the bandwidths for power output (h_P) and wind speed (h_u). For the first conditional moment, we can calculate the weighted average of the power output increments using equation (10).

$$\hat{M}_P^{(n)}(P, u, \tau_m) = \sum_{i=1}^{N-m} (\Delta_{\tau_m} P_i)^n \cdot \frac{K_{a,b}\left(\frac{P_i - P}{h_P}, \frac{u_i - u}{h_u}\right)}{\sum_{j=1}^{N-m} K_{a,b}\left(\frac{P_j - P}{h_P}, \frac{u_j - u}{h_u}\right)} \quad (10)$$

There are plenty of different kernel functions which are useful for different scenarios. We use a Epanechnikov kernel function (11).

The Epanechnikov, Gaussian, and rectangular kernels are three commonly used kernel functions in non-parametric estimation and smoothing techniques. Each of these kernels has distinct properties that impact their use and the resulting estimation or smoothing outcomes.

Epanechnikov Kernel:

- **Shape:** The Epanechnikov kernel has a flat and symmetric shape resembling a parabola, with its maximum value at the center.
- **Efficiency:** The Epanechnikov kernel is considered efficient, providing accurate estimates with the same amount of data.
- **Tails and Robustness:** It has finite tails, making it more robust to outliers and extreme values.

Gaussian Kernel:

- **Shape:** The Gaussian kernel has a bell-shaped curve, characterized by a smooth and continuous decline in values away from the center.
- **Efficiency:** The Gaussian kernel is mathematically tractable and computationally efficient, especially in high-dimensional problems.
- **Tails and Robustness:** It has infinite tails, making it sensitive to outliers and potentially leading to issues when extreme values are present.

Rectangular Kernel:

- **Shape:** The rectangular kernel has a constant value within a fixed interval and drops abruptly to zero outside that interval.
- **Efficiency:** The rectangular kernel is computationally efficient due to its simple shape and properties.
- **Tails and Robustness:** It does have finite tails but a constant value within the fixed interval, making it less robust to outliers and extreme values towards the edges of the interval.

The choice between these kernels depends on the specific characteristics of the data and the desired properties of the estimation or smoothing procedure. The Epanechnikov kernel is often favored when robustness and efficiency are important, and when a localized smoothing effect is desired. The Gaussian kernel is popular for its smoothness and computational efficiency. The rectangular kernel is suitable when simplicity and computational efficiency are prioritized, but it may not handle outliers or extreme values as effectively as the other kernels.

$$k_E(x) = \begin{cases} 1 - x^2 & , |x| \leq 1 \\ 0 & , |x| > 1 \end{cases} \quad (11)$$

At least as important as the kernel function is the related bandwidth. For the analysis of large structures (macro-scale structures), large bandwidths should be used. However, with larger bandwidths, the small structures (micro-scale structures) are no longer visible. To estimate the Kramers-Moyal coefficient of our specific dataset, we used the bandwidths according to the IEC 61400-12-1 [4]. The bandwidth h_u for the wind speed is 1 m/s, and the bandwidth for the power h_P is 100 kW. These bandwidths should be adjusted based on the given dataset (larger bandwidths for a smaller dataset, smaller bandwidths for a larger dataset). For the dataset we used, we found that these bandwidths, in conjunction with the Epanechnikov kernel, yield sensible results.

We assume that the conditional moments $M^{(1)}(P, u, \tau)$ are linear for small time steps τ and that there is no additional measurement noise, i.e., $M^{(n)}(P, u, \tau = 0) = 0$. We can estimate the Kramers-Moyal coefficients using the given estimations of the n -th conditional moments, which are obtained by averaging the conditional moments divided by the used time step τ_m , as shown in Equation (12).

$$\hat{D}_P^{(n)}(P, u) = \frac{1}{M} \sum_{m=1}^M \frac{\hat{M}^{(n)}(P, u, \tau_m)}{n! \cdot \tau_m} \quad (12)$$

In this contribution, we utilize a parametric ansatz to model the system dynamics, where the coefficients $\alpha_i(u)$ depend on the wind speed u . This approach allows us to express the drift term $\tilde{D}_P^{(n)}(P, u)$ as a polynomial function of P with coefficients that vary with u . The parametric ansatz is formulated as:

$$\tilde{D}_P^{(n)}(P, u) = \sum_{i=0}^N \alpha_i(u) \cdot P^i \quad (13)$$

By employing this parametric ansatz, we can determine the stable fixed points $P_0(u)$ of the system [5]. These fixed points correspond to values of P at which the drift term becomes zero, indicating an equilibrium state. Mathematically, this can be expressed as:

$$\tilde{D}_P^{(n)}(P_0, u) = 0 \quad (14)$$

Furthermore, in order to assess the stability of these fixed points, we examine the derivative of the drift at the fixed point. If the derivative is negative, it signifies that the fixed point is stable. More precisely:

$$\frac{d}{dP} \tilde{D}_P^{(n)}(P_0, u) < 0 \quad (15)$$

The derivative of the drift at the fixed point plays a crucial role in understanding the stability of the fixed point as well as providing valuable insights into the mean reversal time. By examining this derivative, we can gain a deeper understanding of the dynamics and behavior of a system around its equilibrium.

When studying the stability of a fixed point, we are interested in how the system responds to small perturbations from its equilibrium state. The derivative of the drift provides information about the local behavior of the system near the fixed point. Specifically, it characterizes the linearization of the dynamics around the equilibrium and reveals important properties such as stability, instability, or the presence of limit cycles.

As said before, if the derivative of the drift evaluated at the fixed point is negative-definite, it indicates that the fixed point is stable. In this case, any small disturbances from the equilibrium will eventually dampen out, and the system will return to its steady state. On the other hand, if the derivative is positive-definite, it suggests that the fixed point is unstable, and even the slightest perturbations will cause the system to diverge away from the equilibrium.

Additionally, the derivative of the drift can provide insights into the mean reversal time of a system. Mean reversal time refers to the average duration it takes for a perturbed system to return to its equilibrium state.

In summary, the derivative of the drift at the fixed point serves as a valuable tool for assessing the stability of the equilibrium and understanding the mean reversal time of a dynamical system. Its analysis provides crucial insights into the local behavior and long-term dynamics, aiding researchers in predicting and understanding the behavior of complex systems in various scientific fields, including physics, biology, economics, and engineering.

3.3 Separation per operational state

We make the assumption that the operational states $S(t)$ of the wind turbine can only take discrete values, specifically $S(t) \in [1, 2, 3, 4, 5]$. Furthermore, we consider that both the drift and diffusion coefficients depend on the turbine's operational state. By incorporating this additional condition, we can reformulate the Langevin equation for the power conversion process using the equation (16).

$$\dot{P}(t)|_{u(t)=u, S(t)=S} = D_P^{(1)}(P(t), u, S) + \sqrt{D_P^{(2)}(P(t), u, S)} \cdot \Gamma(t) \quad (16)$$

The numerical approach can be derived in a similar manner as for the approach for no separation per operational state. The only distinction is that we employ a 3-dimensional Kernel $K_{a,b,c}(x, y, z) = k_a(x) \cdot k_b(y) \cdot k_c(z)$. Due to the discrete values of the operational state, we can utilize a dedicated Boolean kernel function, as shown in Equation (17).

$$k_{\text{Bool}}(x) = \begin{cases} 1 & x = 0 \\ 0 & x \neq 0 \end{cases} \quad (17)$$

We use (18) to estimate the n 'th conditional moment at a specific state (P, u, S) .

$$\hat{M}_P^{(n)}(P, u, S, \tau_m) = \sum_{i=1}^{N-m} (\Delta_{\tau_m} P_i)^n \cdot \frac{K_{a,b,\text{bool}}\left(\frac{P_i-P}{h_P}, \frac{u_i-u}{h_u}, S_i-S\right)}{\sum_{j=1}^{N-m} K_{a,b,\text{bool}}\left(\frac{P_j-P}{h_P}, \frac{u_j-u}{h_u}, S_j-S\right)} \quad (18)$$

The estimation of Kramers-Moyal coefficients follows a similar approach as we have demonstrated previously. However, in this case, we introduce a modified version of the parametric ansatz presented in equation (13). The coefficients $\alpha_i(u, S)$ in this updated ansatz now additionally depend on the state variable S .

The revised parametric ansatz is defined as:

$$\tilde{D}_P^{(n)}(P, u, S) = \sum_{i=0}^N \alpha_i(u, S) \cdot P^i \quad (19)$$

Similar to the previous formulation, the drift term $\tilde{D}_P^{(n)}(P, u, S)$ can be expressed as a polynomial function of P . However, the coefficients $\alpha_i(u, S)$ are now explicitly influenced by both the wind speed u and the state variable S . This allows for a more comprehensive characterization of the system dynamics, additionally taking into account the current state of the system.

By estimating the appropriate values for the coefficients $\alpha_i(u, S)$, we can effectively capture the behavior of the system and quantify its drift as a function of the wind speed, state, and power level.

4 Results

We visualize the nonparametric drift estimation in 1. Here, we can clearly see different deterministic dynamics per operational state. With the parametric ansatz, we were able to calculate the stable fixed points 2 and the corresponding derivatives at the fixed points 3. We find exactly one stable fixed point per operational state and wind speed.

We also visualize the nonparametric diffusion estimation in 4. We can find differences per operational state. We also used the parametric ansatz for the diffusion estimation to calculate the diffusion values at the fixed points which is visualized in 5.

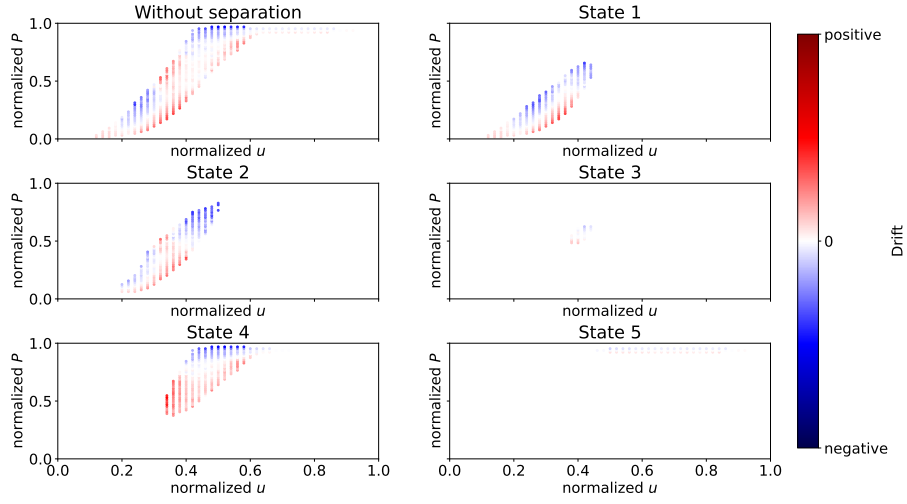


Figure 1: This figure illustrates the drift maps of the power conversion process, categorized by turbine states. The drift values are depicted using a color-coded scheme, with a corresponding colorbar provided on the right-hand side for reference.

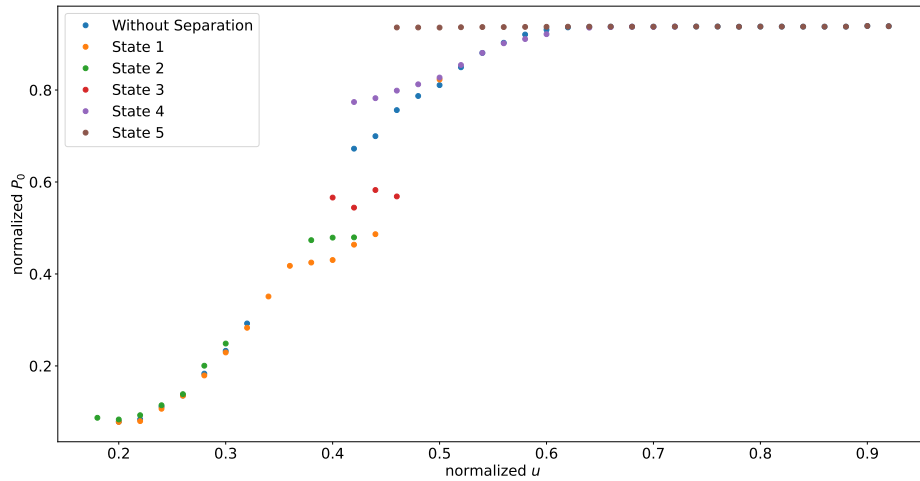


Figure 2: The figure presents a plot showcasing the normalized stable fixed points P_0 of the power output in relation to the normalized wind speed. The fixed points are categorized based on the operational states, with each state distinguished by a distinct color.

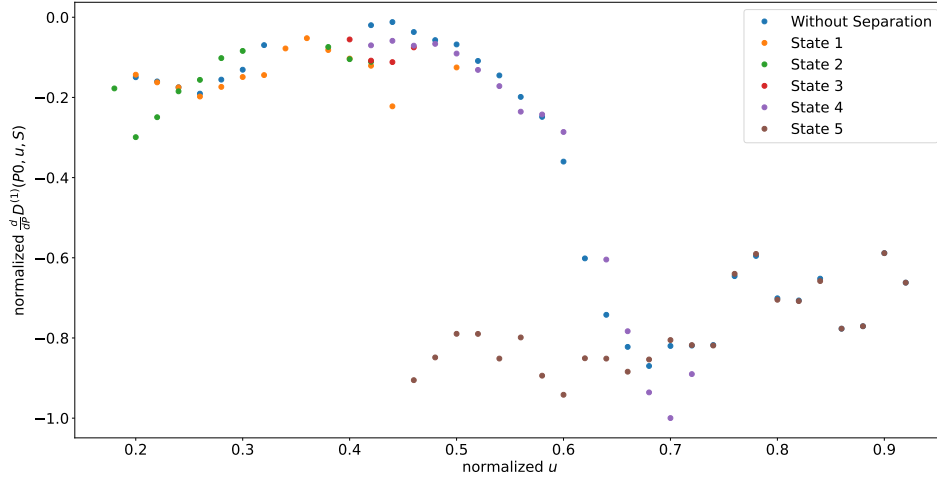


Figure 3: The figure presents a plot showcasing the normalized derivative of the drift at the stable fixed points of the power output in relation to the normalized wind speed. The derivatives are categorized based on the operational states, with each state distinguished by a distinct color.

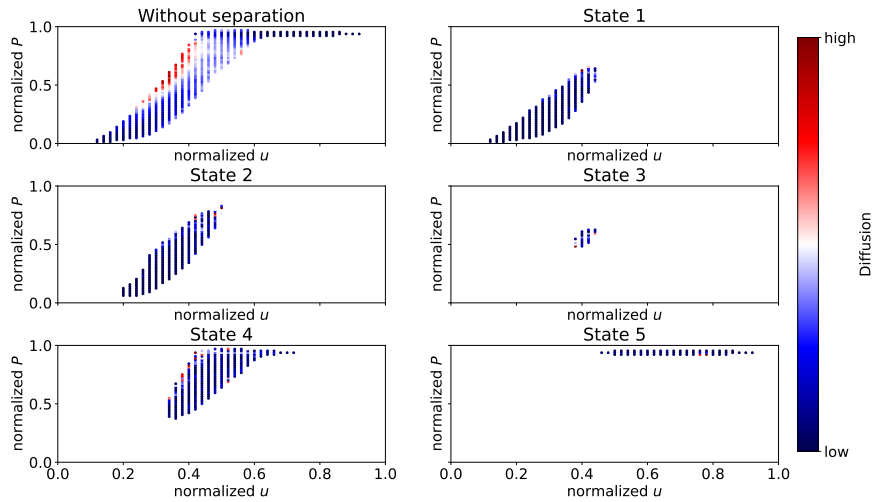


Figure 4: This figure illustrates the diffusion maps of the power conversion process, categorized by turbine states. The diffusion values are depicted using a color-coded scheme, with a corresponding colorbar provided on the right-hand side for reference.

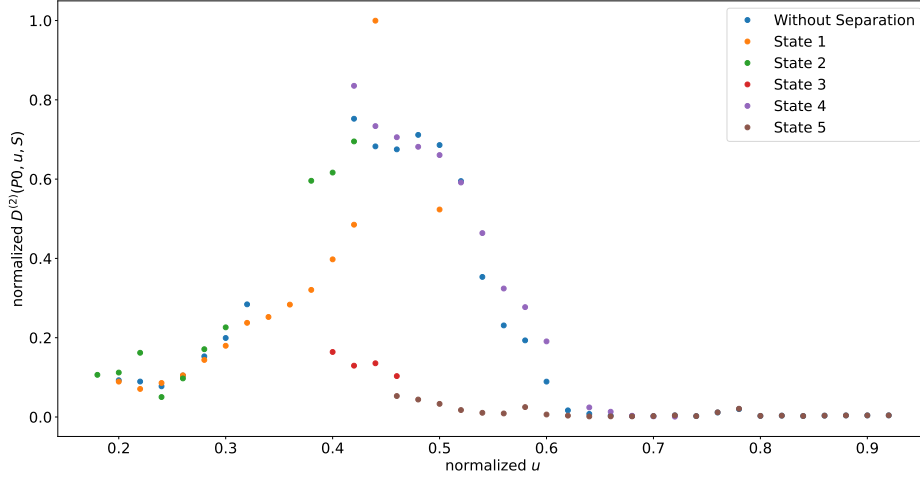


Figure 5: The figure presents a plot showcasing the normalized diffusion values at the fixed points of the power output in relation to the normalized wind speed. The diffusion values are categorized based on the operational states, with each state distinguished by a distinct color.

5 Discussion

Our analysis of the fixed points and the derivative of the drift at the fixed point per wind speed and operational state has revealed a drastic impact of operational states on the system's behavior which is displayed in figure 2 and 3. We have found that different operational states can have a significant influence on the system's stability and long-term behavior. This observation highlights the importance of considering operational states when studying the behavior of the system.

Furthermore, the differences in fixed points between operational states can also explain hysteresis effects that may arise due to switching between states. Hysteresis effects refer to the phenomenon where the system's behavior lags or trails its input, leading to delayed or inconsistent responses. By observing different fixed points in different states, we can gain a better understanding of how the system responds to changes and transitions between states.

In addition to the deterministic behavior, we have also observed significant variations in the stochastic behavior of the system in different operational states. This can be visualized through the diffusion maps, as seen in Figure 4 and the specific diffusion values at the fixed points for each operational state in 5. The diffusion maps highlight the differences in the system's nondeterministic dynamics.

6 Summary

Our analysis has uncovered a range of interesting insights into the behavior of wind turbines under different operational conditions. We have observed significant variations in both the deterministic and stochastic behavior of the system across different states, highlighting the importance of considering operational states when studying the system's behavior.

In terms of deterministic behavior, we have found that the system's dynamics depend between different operational states, as demonstrated by our analysis of the drift maps. We have also observed that different operational states can have a significant impact on the system's stability and long-term behavior, as indicated by our analysis of the fixed points and the derivative at the fixed points per wind speed and operational state.

Moreover, we have observed significant variations in the stochastic behavior of the system in different operational states, as illustrated by our analysis of the diffusion maps.

Overall, our analysis underscores the importance of considering operational states when studying the behavior and performance of wind turbines. By gaining a better understanding of how the system behaves under different conditions, we can optimize its performance and stability.

Acknowledgement

We are grateful to Vattenfall AB for providing the data. This study was carried out in the project Wind farm virtual Site Assistant for O&M decision support – advanced methods for big data analysis (WiSAbigdata) funded by the Federal Ministry for Economic Affairs and Climate Action, Germany (BMWK). One of us (C.P.) thanks for financial support in this project.

References

1. Mücke, T. A., Wächter, M., Milan, P. & Peinke, J. Langevin power curve analysis for numerical wind energy converter models with new insights on high frequency power performance. *Wind Energy* **18**, 1953–1971 (2015).
2. Milan, P., Mücke, T., Morales, A., Wächter, M. & Peinke, J. *Applications of the Langevin power curve* in *Proceedings of the EWE* (2010).
3. Bette, H. M., Jungblut, E. & Guhr, T. Non-stationarity in correlation matrices for wind turbine SCADA-data and implications for failure detection. *Wind Energy Science Discussions*, 1–23 (2021).
4. IEC, I. 61400-12-1 Wind turbines–Part 12-1: Power performance measurements of electricity producing wind turbines. *Geneva, Switzerland: IEC* (2005).
5. Wächter, M., Milan, P., Mücke, T. & Peinke, J. Power performance of wind energy converters characterized as stochastic process: applications of the Langevin power curve. *Wind Energy* **14**, 711–717 (2011).
6. Tabar, R. *Analysis and data-based reconstruction of complex nonlinear dynamical systems* (Springer, 2019).
7. Lin, P. P., Waechter, M., Tabar, M. & Peinke, J. Discontinuous Jump Behavior of the Energy Conversion in Wind Energy Systems. *arXiv preprint arXiv:2301.05553* (2023).